JOURNAL OF MATERIALS SCIENCE **39** (2004) 5081–5089

Mechanically activated synthesis of ultrafine rods of HfB_2 and milling induced phase transformation of monocrystalline anatase particles

S. BÉGIN-COLIN
Laboratoire de Science et Génie des Matériaux et de Métallurgie, C.N.R.S. U.M.R. 7584, Ecole des Mines, F-54042 Nancy Cedex, France

G. LE CAËR
Groupe Matière Condensée et Matériaux, C.N.R.S. U.M.R. 6626, Université de Rennes-I, Campus de Beaulieu, Bâtiment 11A, F-35042 Rennes Cedex, France
E-mail: gerard.le-caer@univ-rennes1.fr

E. BARRAUD, O. HUMBERT
Laboratoire de Science et Génie des Matériaux et de Métallurgie, C.N.R.S. U.M.R. 7584, Ecole des Mines, F-54042 Nancy Cedex, France

The mechanically activated synthesis of hafnium diboride HfB_2 from partially hydrated hafnium tetrachloride "$HfCl_4$" is first described. Monocrystalline rods with submicron to micron lengths and a diameter of about 100 nm are synthesized by annealing, at 1373 K, of powder mixtures of "$HfCl_4$" and boron ground with steel tools. The monocrystalline rods grow parallel to the *c*-axis of the HfB_2 structure from iron-rich grains of the activated powder and are defect-free. Facetted nanometer-sized single crystals are obtained instead when magnesium is added to the starting mixtures. The fractureless transformation of single-crystal anatase particles with different initial sizes into orthorhombic TiO_2-II by milling is then described. Milling yields either monocrystalline anatase particles coated with a layer of nanograins of TiO_2-II (grain size ~10 nm) or fully transformed anatase particles according to the initial diameters of ~150 nm and ~25 nm respectively. The relevance of a milling parameter, namely the average power injected per unit volume of powder trapped during a collision, is finally emphasized.

1. Introduction

The versatility of high-energy ball-milling [1–6] stems from a fortunate combination of technical simplicity and of complexity both of phenomena occurring during grinding and of mechanosynthesized materials. The complexity of mechanisms at work during high-energy ball-milling makes of this technique either a direct method of synthesis of sophisticated materials or a major step, namely mechanical activation [1–6], on the route to such materials. The latter include, among many others, BN nanotubes prepared first by grinding boron powders in NH_3 and subsequently heating in a nitrogen atmosphere [7]. Grinding is seldom recognized to be a possible step in the preparation of nanosized or ultrafine single crystals or to be a way of transforming a part of a single crystalline particle without damaging the whole of it. The present paper focuses on these particular aspects of high-energy ball-milling, namely on the mechanically activated synthesis of ultrafine single crystals of hafnium diboride [8] and on a phase transformation induced by milling either at the surface or in the bulk of single-crystalline particles of anatase TiO_2 according to their initial size, ~25 nm or ~150 nm respectively [9–11].

2. Mechanically activated synthesis of HfB_2 nanorods

Metal diborides MB_2, more particularly those made from transition metals, for instance M = Ti, Zr, Nb, Mo, Hf, Ta, have high melting points (~3000 K), high hardness (some tens of GPa) and high electrical and thermal conductivities (~0.1 $\mu\Omega$ m and some tens of W/mK respectively for M = Ti). They are of interest among others in the fields of cutting tools, reinforcement of ceramics and metals, coating materials, electron emitters and heterogeneous catalysis. However the high melting points of these diborides makes it difficult to produce single-phased materials. The recent discovery of bulk superconductivity in MgB_2 [12] has been a great boost to the development of synthesis methods, to microstructural characterization and to theoretical and experimental studies of this diboride and of related compounds, more particularly those with the AlB_2 type structure.

The latter structure is hexagonal (space group P6/mmm with one formula unit per unit cell) and consists simply in a repeated stacking of a graphite-like boron layer and of a close-packed Al layer in the *c*-direction. Space is thus filled by triangular prisms of Al atoms whose centres are occupied by boron atoms.

Mechanical alloying (MA) has been widely used to synthesize borides by high energy ball-milling of elemental powder mixtures followed or not by annealing treatments [13–22]. In some cases these reactions may be highly exothermic and of combustive or SHS type. Another route consists in milling mixtures of oxide and boron powder and in annealing ground powders [20] with the eventual addition of a reducing element which is further extracted by leaching [21, 22].

In the present work, single crystals of HfB_2 were synthesized either in the form of rods with submicron to micron lengths and nanometer-sized diameters or in the form of facetted submicron crystals respectively from $HfCl_4 + B$ and from $HfCl_4 + B + Mg$ powder mixtures that were first mechanically activated by high-energy ball-milling and then annealed at 1373 K under argon atmosphere for 1 h.

2.1. Experimental conditions

The weights of B and Mg in the initial powder mixtures were in excess of 100% at the most with respect to those obtained from the following reactions:

$$HfCl_4 + 2B + 2Mg \rightarrow HfB_2 + 2MgCl_2 \quad \text{and}$$

$$HfCl_4 + 10/3B \rightarrow HfB_2 + 4/3BCl_3$$

"$HfCl_4$" is a very hygroscopic compound whose composition is actually $\sim x HfCl_4 - (1-x)HfOCl_2 - 2(1-x)HCl - nH_2O$ ($0 \leq n \leq 8$) (with a decrease of n from the periphery to the center of particles) [8]. The powder mixtures were milled in a planetary ball-mill (Fritsch Pulverisette 7), with a disc rotation speed of about 710 rpm, using seven steel (with ~4.5 at.% C and 1.5% Cr) balls and steel (with ~6.7 at.% C and 12 at.% Cr) vials. The powder-to-ball weight ratio was 1/20 and all milling experiments were carried out without interruption under an argon atmosphere for times of 8 h at the most. ^{57}Fe Mössbauer spectra showed that the Cr content of α-Fe in the as-milled powders is only consistent with a predominant contamination by steel from balls. The various phases were identified from X-ray diffraction patterns. The powders were observed with a scanning electron microscope (SEM) and with a transmission electron microscope equipped with an energy dispersive spectroscopy system for composition analysis and with an electron energy loss spectroscopy system.

Thermogravimetric analyses of ground powders were performed under argon: powders were heated to various temperatures with a heating rate of 5 K/min, then annealed isothermally for one hour and then cooled down to room temperature. Unless otherwise stated, the standard synthesis conditions considered below are milling for 2 h with an excess of reactants of 100% followed by annealing for 1 h at 1373 K. Controlled rate thermal analysis and infrared spectroscopy under vacuum were further used to investigate the evolution of ground powders when heated.

2.2. Synthesis of single crystalline HfB_2

2.2.1. From "$HfCl_4$" + B + Mg starting mixtures

As-prepared powder mixtures were annealed for 1 h under argon at various temperatures ranging between 773 and 1373 K. The diffraction lines of Hf, HfO_2, $MgCl_2{\cdot}6H_2O$, MgO are observed after annealing at 773 K but those of the starting "$HfCl_4$" are absent. The powders annealed at 1373 K consists of HfB_2 (65 wt%), HfO_2 (monoclinic, 11 wt%) and MgO (24 wt%). The thermal decomposition of "$HfCl_4$" yields HfO_2 while Hf is predominantly formed by the reduction of "$HfCl_4$" by Mg as shown by the presence of $MgCl_2{\cdot}6H_2O$. Another possible source of Hf is a partial reduction of HfO_2 by Mg at high temperature [8]. Boron reacts with Hf and HfO_2 to form the diboride.

As-prepared mixtures are significantly contaminated by steel during milling (about 13 wt% in the standard conditions defined in Section 2.1). After milling, X-ray diffraction patterns of ground mixtures show the presence of $MgCl_2{\cdot}6H_2O$, HfH_x ($1.6 < x < 2$), bcc Fe, MgO and a weak contribution from HfB_2. Infrared spectroscopy further indicates the formation of boron oxides or (/and) boron hydroxides and that of a compound formed by hydrolysis of $MgCl_2$ [8]. Hafnium hydrides are also observed to form during milling of a mixture of "$HfCl_4$" and of Mg. Milled powders are made of microsized particles whose inner part is rich in Hf and B while their outer part is rich in Mg, Cl and O. The main phases in powders annealed at 1373 K are HfB_2, MgO, FeB and an hafnium oxide with an oxygen content of about half that of hafnia, possibly isotypic with metastable cubic zirconium monoxide ZrO [23]. The optimum synthesis conditions, which yield the maximum amount of HfB_2, consist in milling for one 1 h a mixture whose B and Mg constituents are in a 50 wt% excess. In that way, the Fe contamination is decreased to about 4 wt%. The relative weights of HfB_2, HfO_2 and of MgO in ground powders annealed for 1 h at 1373 K are 0.81, 0.06 and 0.13, respectively. Facetted grains of HfB_2, with an average size of about 300 nm, are observed in the latter powders (Fig. 1a).

2.2.2. From "$HfCl_4$"+B starting mixtures

The optimized milling and annealing conditions are the same as those described above, namely milling for 1 h with B in excess by ~50% followed by annealing for 1 h at 1373 K. X-ray diffraction patterns of milled powders show broad lines attributed to the starting "$HfCl_4$" and to bcc Fe from milling tools. Mössbauer spectrometry further shows the presence of $FeCl_2$ establishing that Fe takes part in a partial reduction of "$HfCl_4$" during milling while infrared spectroscopy proves that boron reacts with water and with hafnium oxychloride. After annealing, the hafnium phases are HfB_2 and HfO_2 (monoclinic form) with relative weights of 0.92 and

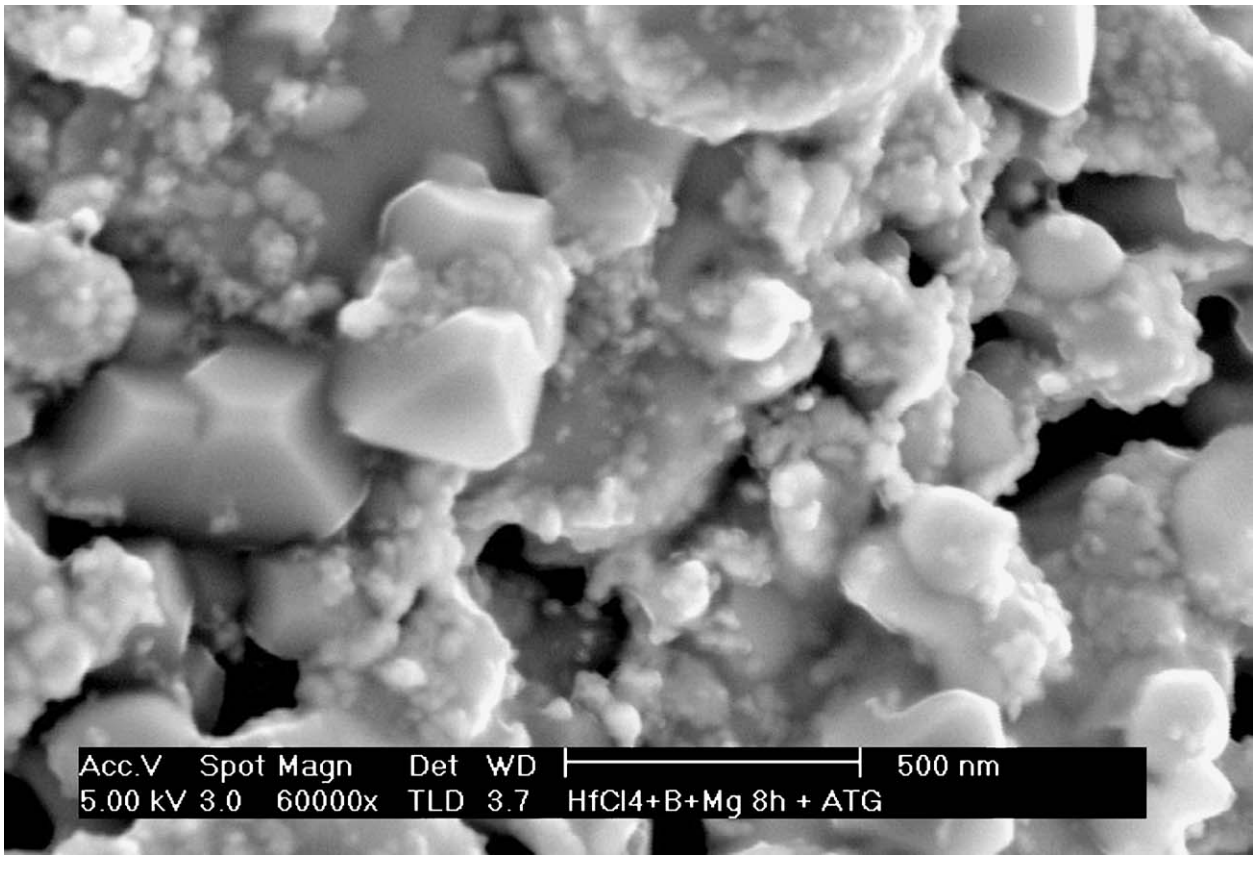

(a)

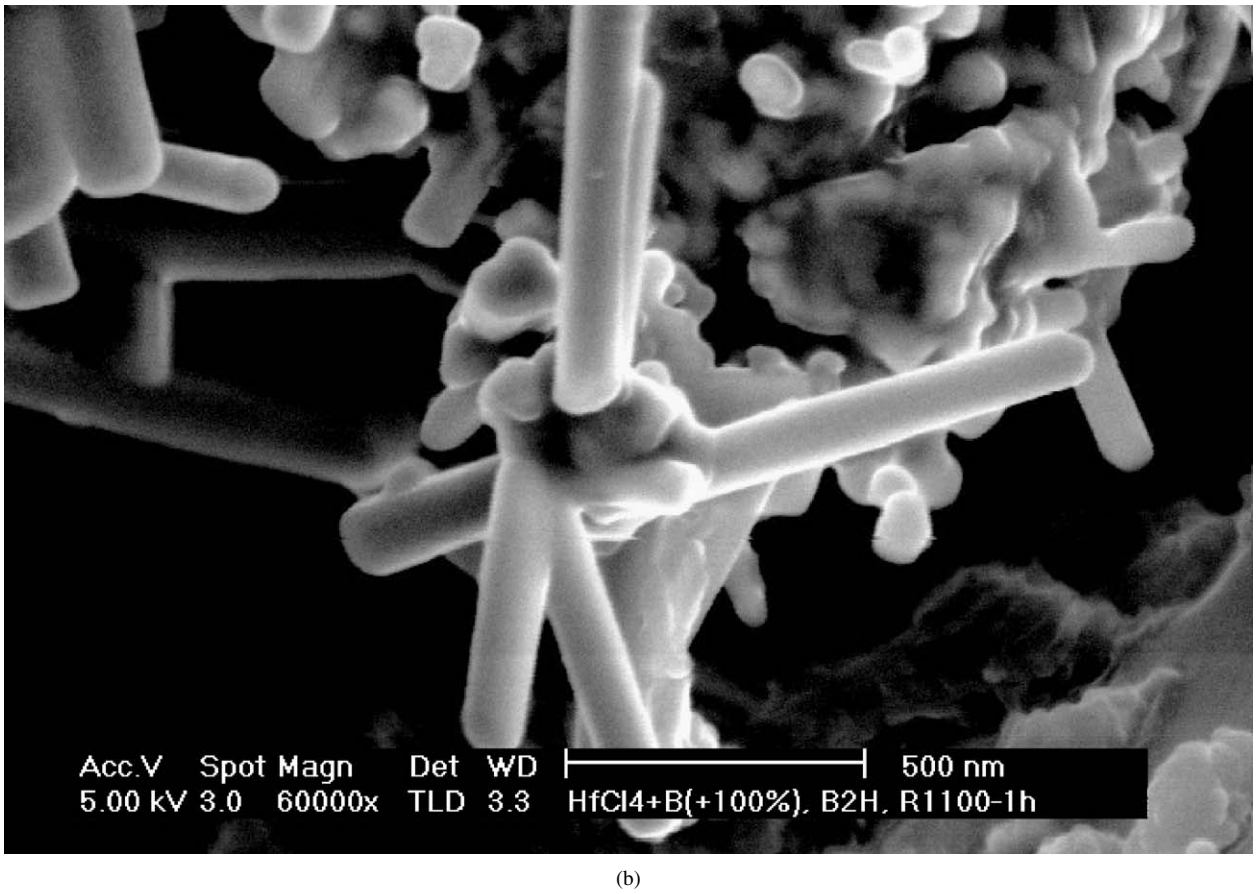

(b)

Figure 1 Scanning electron micrographs of HfB_2 prepared from powder mixtures mechanically activated for 2 h and annealed for 1 h at 1373 K (a) facetted crystals formed from a mixture of "$HfCl_4$", Mg and B (b) nanorods formed from a mixture of "$HfCl_4$" and B.

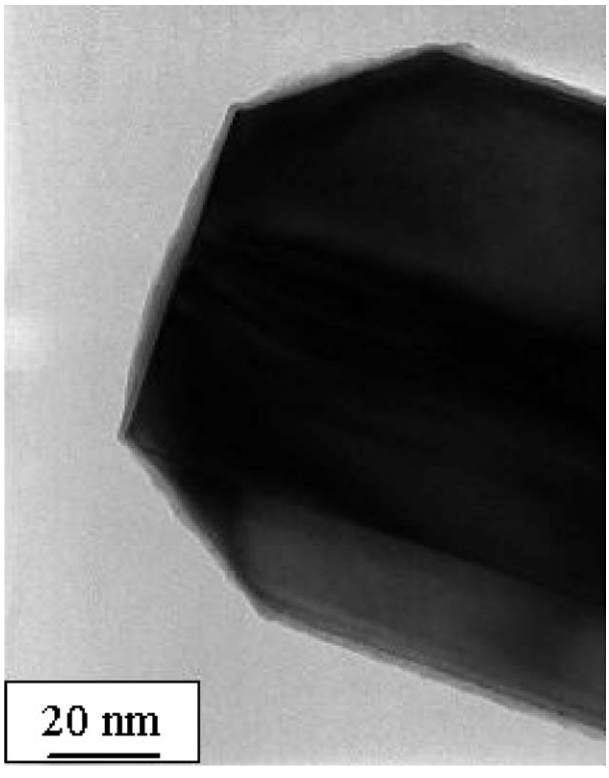

Figure 2 Transmission electron micrograph of a facetted tip of a HfB_2 nanorod (its diameter is about 100 nm and its longitudinal axis is parallel to the *c* axis).

0.08 respectively, while the main iron phase FeB, with its low and high temperature modifications, represents approximately 5% of the total weight. Phase evolution at 1373 K, which was followed as a function of annealing time, proves that HfB_2 forms from HfO_2 which comes from the thermal decomposition of "$HfCl_4$" [8].

Monocrystalline rods of HfB_2, with facetted tips and a thin oxide passivation layer (∼3 nm), are synthesized in such conditions (Figs 1b and 2).

The monocrystalline rods, with diameters ranging between 50 and 100 nm and lengths of ∼1 μm, grow parallel to the *c*-axis of the HfB_2 structure ($c =$ 0.352 nm) from grains of the activated powder rich in Hf, B, Fe and O (Fig. 1) and are defect-free [8]. The formation of nanorods is observed too when ZrB_2 is prepared in similar conditions from "$ZrCl_4$". The mechanochemical synthesis of TiB_2 from $TiO_2 + B_2O_3 +$ graphite mixtures yields similarly monocrystalline nanorods [22].

The influence of various parameters on the nanorod growth was investigated [8]. The synthesis of HfB_2 from HfO_2 seems to be a necessary condition to produce that kind of morphology which is not observed when the diboride is formed from the direct boridation of Hf (Section 2.2.1). Supplementary conditions are mechanical activation and Fe contamination. Annealing of an as-prepared mixture of "$HfCl_4$" + B + Fe gives rods with an heterogeneous size distribution and a low yield, as exemplified by Fig. 3, and proves that the mixing and the activation brought up by milling are moreover needed. A low nanorod yield is found too for as-prepared mixtures of HfO_2 + B + Fe. Finally, the presence of molten boron oxide may influence the diffusion of reactants while vapour liquid solid mechanisms involving boron oxide vapours may occur.

3. Fractureless transformation of ground anatase TiO_2

Nanosized oxide powders synthesized or activated by high-energy ball-milling may be of great interest in numerous fields such as catalysis or manufacturing of materials with enhanced mechanical properties. Titanium dioxide occurs in nature in three crystalline phases: anatase, brookite and rutile. Other polymorphs, which are formed in equilibrium conditions at high-pressure and at high-temperature or in non-equilibrium conditions, for instance by high-energy ball-milling of anatase [9–11, 24–28] or by laser irradiation [29], include the orthorhombic α-PbO_2 type-structure, often called TiO_2-II, whose transformation conditions depend further on size for nanometer-sized crystals [24, 28, 29]. The phase boundary between rutile and TiO_2-II, when plotted in a pressure-temperature diagram, was observed to be shifted towards lower pressure for nanophase materials [28, 29].

The polymorphic transformation of anatase into TiO_2-II induced by high-energy ball-milling yields unusual ground materials, stresses the role of mechanical properties of milled materials and evidences the relevance of a milling parameter, namely the average power injected per unit volume of powder trapped during a collision [30].

3.1. Experimental conditions

Grinding experiments described below were performed in air with a powder to ball weight ratio of 1/30 and milling conditions otherwise similar to those described in Section 2.1. Two types of as-received TiO_2 powders were milled. The first is a powder made of monocrystalline particles with an average diameter of ∼25 nm, labeled TiO_2(A) in the following, containing mainly the anatase phase and around 18% in volume of rutile. The second powder, labeled TiO_2(B), whose particles are single-crystals with an average diameter of ∼150 nm, contains around 3% in volume of rutile. The results of milling experiments of TiO_2(B) performed with tools made of different materials (alumina, zirconia, steel) for various disc rotation speeds and powder to ball weight ratios are reported in [30, 31].

3.2. Main features of the transformation: Milled anatase → TiO_2-II

The anatase volume fraction in ball-milled TiO_2 decreases with milling time, that of rutile increases while that of TiO_2-II reaches a maximum and then decreases [10, 11]. Two reactions occur consecutively: anatase → TiO_2-II → rutile. The maximum volume fraction of TiO_2-II in both powders is achieved after grinding for about 25 min. However it is smaller for the TiO_2(A) powder, 49 vol%, than for the TiO_2(B) one, 68 vol%. In the same way, the rutile volume fraction increases right from the start of grinding in ground TiO_2(A) powder

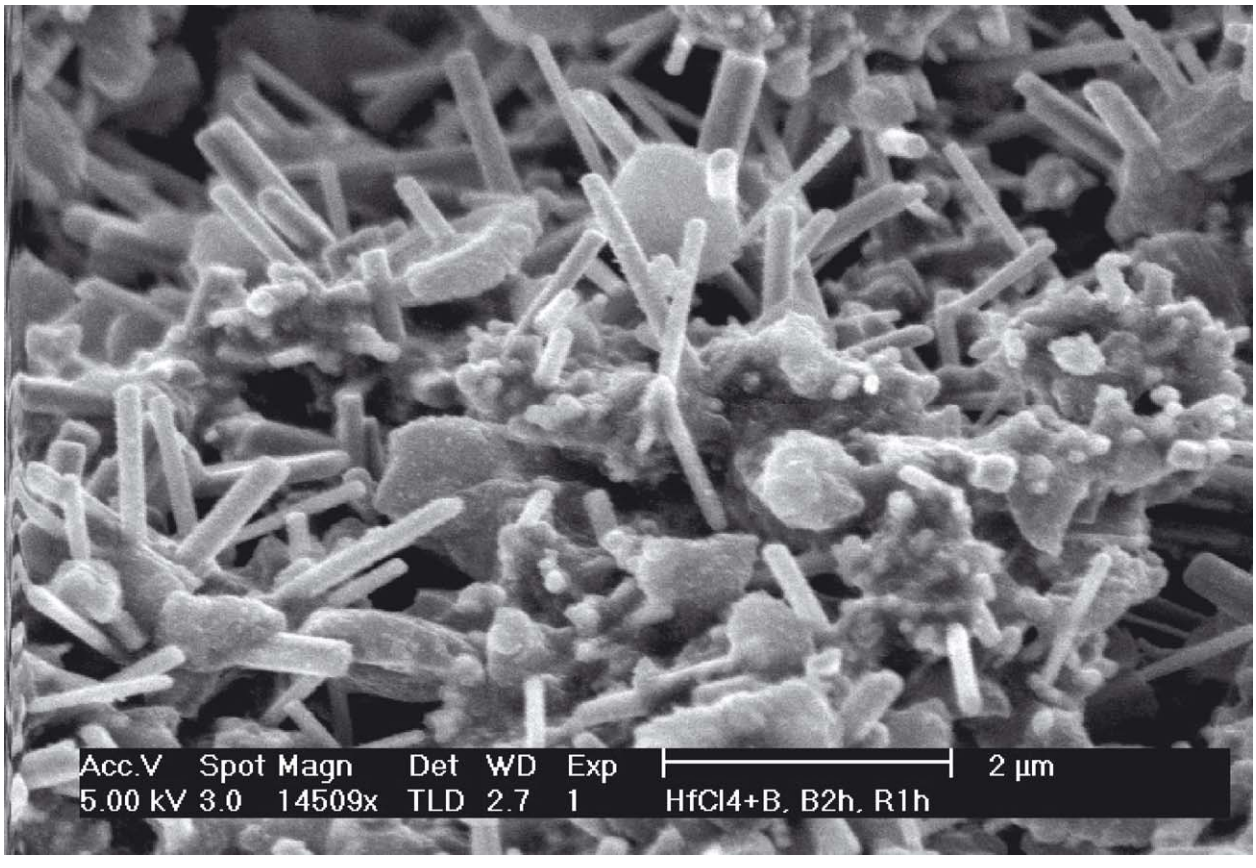

(a)

(b)

Figure 3 Scanning electron micrographs of powder mixtures annealed for 1 h at 1373 K (a) "$HfCl_4$" + B mixture mechanically activated for 2 h (b) as-prepared "$HfCl_4$" + B + Fe mixture.

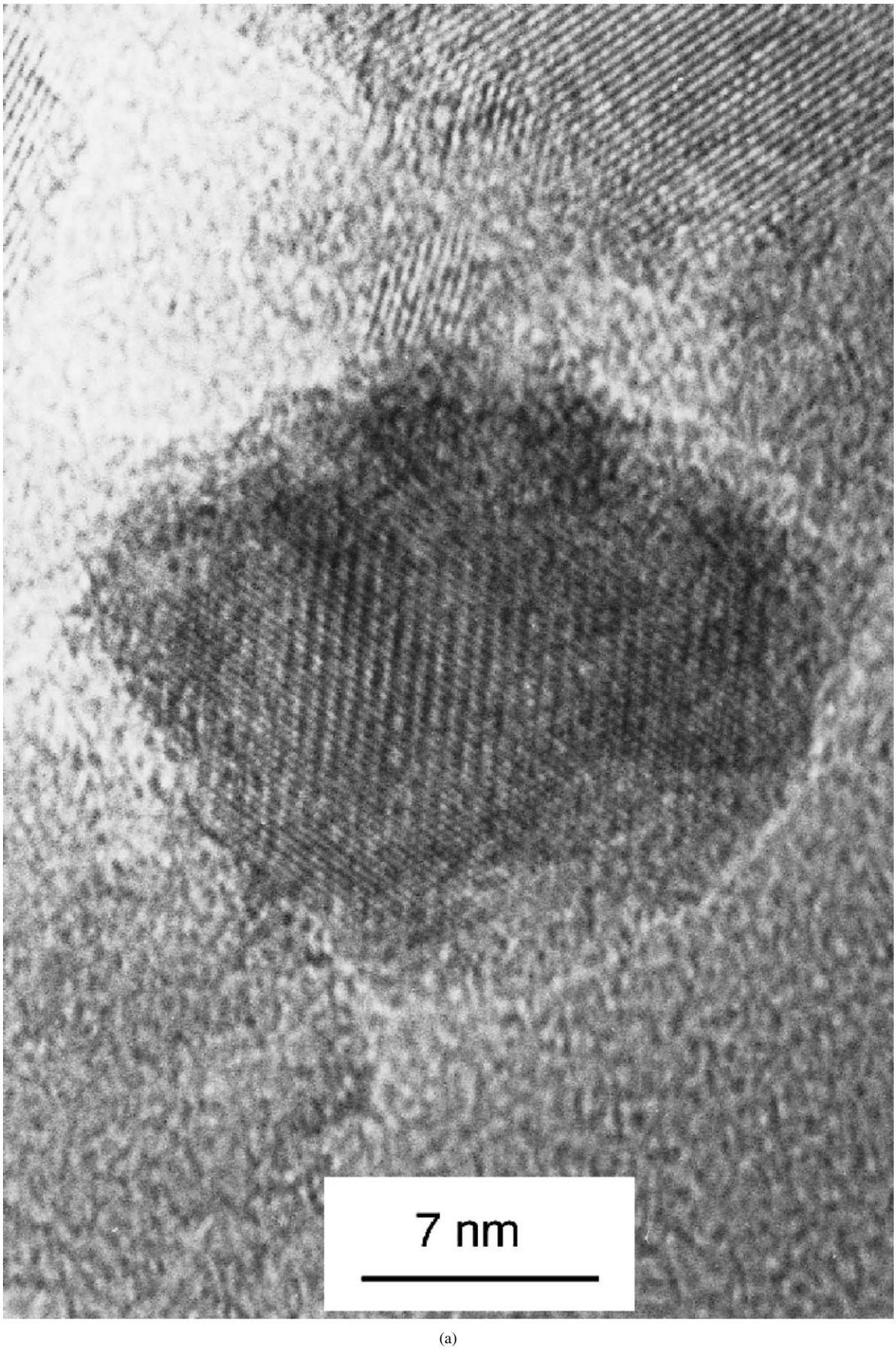

(a)

Figure 4 TEM micrographs (a) of a particle of the as-received TiO_2(A) powder and (b) of a TiO_2-II nanograin from ground TiO_2(B). (*Continued*)

(b)

Figure 4 (*Continued*)

while it increases only after a delay of ∼12 min for the TiO_2(B) one. The significant fraction of rutile in the starting TiO_2(A) powder might have a catalytic effect on rutile formation.

The typical room-temperature compressive strength of coarse-grained TiO_2 is 900 MPa. The formation of metastable TiO_2-II occurs during the first minutes of milling and up to at least 30 min *without fracture of anatase particles* for both TiO_2 (A, B) powders as deduced from particle size and specific area measurements, from scanning and from TEM observations of ground powders [10, 11, 24, 30, 31].

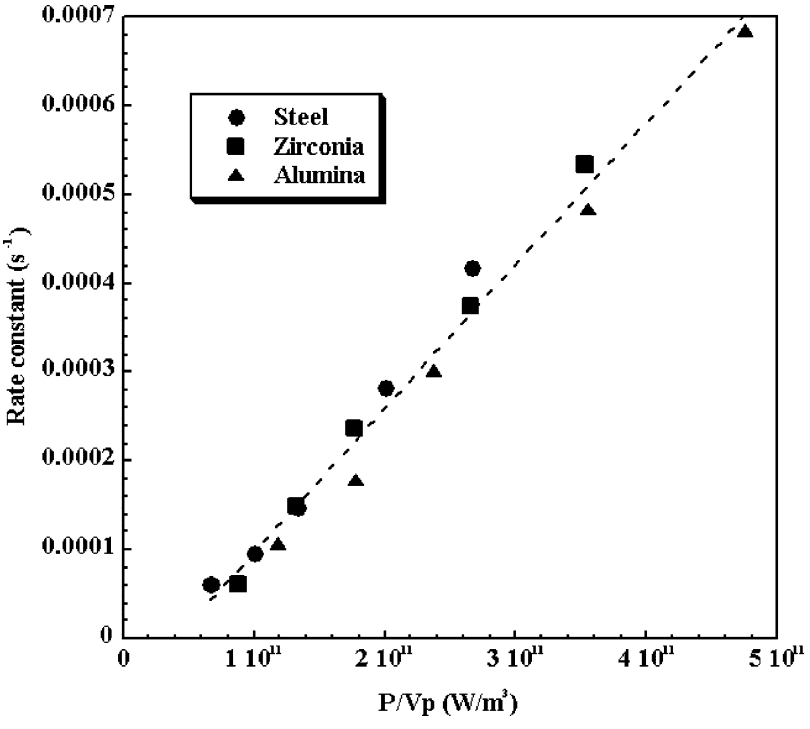

Figure 5 Rate constant of the anatase → TiO_2-II phase transformation as a function of the power transferred by unit volume of trapped powder.

TEM studies of ground TiO_2(B) powders [11] have demonstrated that TiO_2-II crystallites with diameters around ten nanometers form at the surface of anatase particles (Fig. 4) which are thus coated with a TiO_2-II superficial layer which thickens regularly with milling time. The core of anatase particles is simultaneously strain-hardened. During each shock, TiO_2-II nanograins form at the contact points between trapped particles if the local forces are high enough [11, 31]. By contrast, a similar study performed with the TiO_2(A) powder [24] (Fig. 4) shows that TiO_2-II nanograins are not observed to form at the surface of these small anatase particles. Single particles of TiO_2-II, with a diameter in the range 10–20 nm, are instead found inside the bulk of ground powders [24]. Ground TiO_2(A) particles exhibit an intrinsic surface roughness in contrast to TiO_2(B) powders whose roughness is due to TiO_2-II nanograins formed at the surface of anatase particles (Fig. 4) [11]. Zeta potential measurements and adsorption isotherms have shown that grinding induces modifications of the surface properties of TiO_2(A) particles [24].

For all investigated milling conditions of TiO_2(B), the rate constant k of the transformation was obtained for instance from the fraction f of anatase remaining after short milling times t_m: $f \propto (1 - (1 - k \cdot t_m)^3)$. Local models based on the Hertz impact theory were used to evaluate the powder volume V_p trapped between two colliding balls or between a ball and a vial wall, the maximum contact pressure, the contact radii, etc. [31]. A unique linear dependence (Fig. 5) was found whatever the milling conditions and the milling materials only when k was plotted versus the average power injected per unit volume of powder trapped during a collision [30]. The latter milling parameter appears physically meaningful because the evolution of ground particles takes place essentially in aggregates of particles, dynamically confined during shocks, whose average volume is estimated to be here of the order of $5 \cdot 10^{-10}$ m^3.

4. Conclusion

The capabilities of high-energy ball-milling to activate the synthesis of monocrystalline materials and to transform single-crystalline particles without damaging them have been exemplified by the synthesis of ultrafine rods of hafnium diboride and of TiO_2-II. Contamination by steel milling tools is not always detrimental or without influence. It may be beneficial, particularly when Fe-rich nanoparticles help to catalyze reactions during annealing of mechanically activated powders. Milling is nowadays a modern technique of preparation and of transformation of materials, often with original features, which turns simple mills into true reactors [1–6, 32]. Further, mechanosynthesis is a step in the preparation of consolidated materials with improved properties [32].

References

1. V. V. BOLDYREV, N. Z. LYAKHOV, YU. T. PAVLYUKHIN, E. V. BOLDYREVA, E. YU. IVANOV and E. G. AVVAKUMOV, *Sov. Sci. Rev. B. Chem.* **14** (1990) 105.
2. B. S. MURTY and S. RANGANATHAN, *Int. Mater. Rev.* **43** (1998) 101.
3. E. GAFFET, F. BERNARD, J. C. NIEPCE, F. CHARLOT, C. GRAS, G. LE CAËR, J. L. GUICHARD, P. DELCROIX, A. MOCELLIN and O. TILLEMENT, *J. Mater. Chem.* **9** (1999) 305.
4. C. SURYANARAYANA, *Progr. Mater. Sci.* **46** (2001) 1.
5. L. TAKACS, *ibid.* **47** (2002) 355.
6. T. GRIGORIEVA, M. KORCHAGIN and N. LYAKHOV, *Kona* **20** (2002) 144.
7. Y. CHEN, J. FITZ GERALD, J. S. WILLIAMS and S. BULCOCK, *Chem. Phys. Lett.* **299** (1999) 260.

8. E. BARRAUD, Ph.D. Thesis, Institut National Polytechnique de Lorraine, Nancy (2003); E. BARRAUD, S. BÉGIN-COLIN and G. LE CAËR (2003) in preparation.
9. S. BÉGIN-COLIN, G. LE CAËR, A. MOCELLIN and M. ZANDONA, *Phil. Mag. Lett.* **69** (1994) 1.
10. S. BÉGIN-COLIN, T. GIROT, G. LE CAËR and A. MOCELLIN, *J. Solid State Chem.* **149** (2000) 41.
11. T. GIROT, X. DEVAUX, S. BÉGIN-COLIN, G. LE CAËR and A. MOCELLIN, *Phil. Mag.* A **81** (2001) 489.
12. J. NAGAMATSU, N. NAKAGAWA, T. MURANAKA, Y. ZENITANI and J. AKIMITSU, *Nature* **410** (2001) 63.
13. A. CALKA and A. P. RADINSKI, *J. Less-Common Met.* **161** (1990) L23.
14. M. A. MORRIS and D. G. MORRIS, *J. Mater. Sci.* **26** (1991) 4687.
15. Y. PARK, T. HASHIMOTO, T. ABE, R. WATANABE and T. MASUMOTO, *Mater. Sci. Eng.* A **181/182** (1994) 1291.
16. A. CORRIAS, G. ENNAS, G. MARONGIU, A. MUSINU, G. PASCHINA and D. ZEDDA, *ibid.* **204** (1995) 211.
17. L. TAKACS, *Mater. Sci. Forum* **225–227** (1996) 553.
18. K. KUDAKA, K. IUZUMI and T. SASAKI, *J. Ceram. Soc. Jpn.* **107** (1999) 101.
19. K. KUDAKA, K. IIZUMI, T. SASAKI and S. OKADA, *J. Alloys Compd.* **315** (2001) 104.
20. P. MILLET and T. HWANG, *J. Mater. Sci.* **31** (1996) 351.
21. N. J. WELHAM, *J. Amer. Ceram. Soc.* **83** (2000) 1290.
22. *Idem., Metall. Mater. Trans.* A **31** (2000) 283.
23. X. ZHE and A. HENDRY, *J. Mater. Sci. Lett.* **17** (1998) 687.
24. S. BÉGIN-COLIN, G. LE CAËR, F. VILLIERAS, X. DEVAUX, M. O. SIMONNOT, T. GIROT and P. WEISBECKER, *J. Metastable and Nanocrystalline Mater.* **12** (2002) 27.
25. R. M. REN, Z. G. YANG and L. L. SHAW, *J. Mater. Sci.* **35** (2000) 6015.
26. A. GAJOVIC, M. STUBICAR, M. IVANDA and K. FURIC, *J. Mol. Struct.* **563** (2001) SI-315.
27. P. BOSE, S. K. PRADHAN and S. SEN, *Mater. Chem. Phys.* **80** (2003) 73.
28. J. STAUN OLSEN, L. GERWARD and J. Z. JIANG, *J. Phys. Chem. Sol.* **60** (1999) 229.
29. S. Y. CHEN and P. SHEN, *Phys. Rev. Lett*. **89** (2002) 096106-1.
30. T. GIROT, S. BEGIN-COLIN, X. DEVAUX, G. LE CA Ë R and A. MOCELLIN, *J. Mater. Synth. Process.* **8** (2000) 139.
31. T. GIROT, Ph.D. Thesis, Institut National Polytechnique de Lorraine, Nancy (2001).
32. E. GAFFET and G. LE CAËR, in "Encyclopedia of Nanoscience and Nanotechnology," edited by H.S. Nalwa (American Scientific Publishers, Stevenson Ranch, California, USA, 2004) vol. 5, p. 91.

Received 11 September 2003
and accepted 27 February 2004